DOI: 10.1002/smll.200600489

A Single-Step Photolithographic Interface for Cell-Free Gene Expression and Active Biochips

*Amnon Buxboim, Maya Bar-Dagan, Veronica Frydman, David Zbaida, Margherita Morpurgo, and Roy Bar-Ziv**

We have developed a biochip platform technology suitable for controlled cell-free gene expression at the micrometer scale. A new hybrid molecule, "Daisy", was designed and synthesized to form in a single step a biocompatible lithographic interface on silicon dioxide. A protocol is described for the immobilization of linear DNA molecules thousands of base pairs long on Daisy-coated surfaces with submicrometer spatial resolution and up to high densities. On-chip protein synthesis can be obtained with a dynamic range of up to four orders of magnitude and minimal nonspecific activity. En route to on-chip artificial gene circuits, a simple two-stage gene cascade was built, in which the protein synthesized at the first location diffuses to regulate the synthesis of another protein at a second location. We demonstrate the capture of proteins from crude extract onto micrometer-scale designated traps, an important step for the formation of miniaturized self-assembled protein chips. Our biochip platform can be combined with elastomeric microfluidic devices, thereby opening possibilities for isolated and confined reaction chambers and artificial cells in which the transport of products and reagents is done by diffusion and flow. The Daisy molecule and described approach enables groups not proficient in surface chemistry to construct active biochips based on cell-free gene expression.

Keywords:
- biochips
- cell-free translation
- gene circuits
- nanotechnology
- self-assembled monolayers

[*] A. Buxboim, M. Bar-Dagan, Dr. D. Zbaida, Dr. R. Bar-Ziv
Departments of Materials and Interfaces
The Weizmann Institute of Science
PO Box 26, Rehovot 76100 (Israel)
Fax: (+972) 8934-4137
E-mail: roy.bar-ziv@weizmann.ac.il

Dr. V. Frydman
Chemical Research Support
The Weizmann Institute of Science
PO Box 26, Rehovot 76100 (Israel)

Dr. M. Morpurgo
Biological Chemistry, The Weizmann Institute of Science
PO Box 26, Rehovot 76100 (Israel)

Dr. M. Morpurgo
Pharmaceutical Sciences Department, University of Padova
Via Marzolo 5, 35100 Padova (Italy)

Supporting information for this article is available on the WWW under http://www.small-journal.com or from the author.

1. Introduction

1.1. Motivation

The motivation for this work was to provide a simple biochip platform for exploring artificial systems based on cell-free gene expression. Present DNA and protein biochips have been developed for measuring the abundance of specific biomolecules, for example, through nucleic acid hybridization, and for examining the biochemical function of target proteins localized on a surface.[1–8] In principle, however, biochip methodologies could be extended from passive probe–target interactions to include complex and cascaded activities on the chip. For example, in vitro transcription/translation reactions,[9,10] enzyme catalysis,[11,12] and surface-mediated biorecognition events may all be required to occur

NANO MICRO small

concomitantly at different sites on a single chip. Reaction products could then interact amongst themselves or with other immobilized molecules to perform additional activities. For this purpose, one would need to separately immobilize chemically different entities, such as DNA, proteins, and low-molecular-weight compounds, with submicrometer resolution on the same chip to permit rapid communication by diffusion of the biosynthetic reaction products between sites.

In vitro gene-expression systems are widely used but they are typically carried out in bulk solution. Recently, such systems have been encapsulated in membrane compartments, thereby defining a linkage between genotype and phenotype[13] that can be used for experiments on molecular evolution and the origin of life[14] and for constructing artificial "cells".[15–18] In vitro gene-expression systems can be made more complex by including regulatory elements to create circuits,[19–21] similarly to natural gene networks in living cells. The assembling of such circuits in vitro allows one to investigate their design principles and information flow[19] and to construct novel biochemical, morphogenetic,[20] and computational modules.[21–23] Eventually, this approach may be combined with autonomous devices at the nanoscale.[24–30] However, experiments conducted in homogenous bulk solution or encapsulated in membranes suffer from the limitation that the information-processing units are not localized.

To extend the cell-free gene-expression approach to allow localization of information-processing units, we have developed a surface platform on which biosynthetic reactions can be carried out under controlled conditions. This platform is a first step towards functional cell-free biochemical factories for synthesizing reagents and decision-making modules. Localization of transcription/translation reactions on a surface at the micrometer scale opens the possibility of engineering the inherent length and time scales associated with concentration gradients, which is otherwise impossible in homogeneous bulk solution systems. Placing of the genes in close proximity on a surface facilitates their communication through reaction–diffusion, whereby the gene product synthesized at one location diffuses to interact with another gene, or gene product, located elsewhere. Cell-free transcription/translation originating from localized genes can be coordinated and cascaded in place and in time, similarly to the morphogenetic networks in living organisms.[20,31]

1.2. Approach and Summary

An interface for cell-free gene expression must meet a number of requirements: a) compatibility with biosynthetic reactions; b) a wide dynamic range of activity of the immobilized molecules; c) minimal nonspecific adsorption; d) a sequential immobilization scheme for molecules with different chemical properties at submicrometer resolution; and e) simplicity, robustness, and reproducibility in the hands of groups not proficient in surface chemistry. We present a photolithographic interface on silicon dioxide that fulfills these requirements. Our approach is based on a newly synthesized molecule that forms a biocompatible self-assembled monolayer in a single step.

This paper describes the synthesis of the new molecule and presents its use for surface derivatization together with the characterization of the resulting modified surface. We obtain a homogenous biocompatible dense monolayer on silicon dioxide that has chemically protected amine groups separated by an average distance of 1.6 nm. These amine groups become available for chemical coupling upon exposure to UV light. While the approach is general and applicable for coupling a wide variety of biomolecules, we focused on the light-directed immobilization of linear double-stranded DNA (dsDNA) molecules that are a few thousands of base pairs (bp) long and code for entire genes, in contrast to current DNA chips where only short single-stranded DNA molecules have been immobilized to submicrometer precision. The dsDNA molecules were localized lithographically on the surface at one end through biotin–streptavidin (SA) conjugation. We have obtained a specific-to-nonspecific immobilization ratio as high as $\approx$200 and control of gene density up to a tight packing of 30 nm average distance between neighboring molecules for $\approx$2000 bp dsDNA. Spatial patterning of these long dsDNAs is possible at submicrometer resolution. We find these results meaningful since long dsDNAs are highly charged semiflexible polymers that adsorb nonspecifically and sporadically onto nontreated surfaces.

We carried out protein synthesis from localized dsDNA coding for the reporter gene firefly *luciferase* as a function of dsDNA number and density. Protein production was induced by bathing the chip in a transcription/translation reaction mix. Either of two bacteriophage RNA polymerases, T7 or sp6, was used for transcription, whereas translation was accomplished by using a commercial expression cocktail based on eukaryotic (wheat germ) cell extract in a reconstituted buffer that includes nucleotides, amino acids, tRNAs, and an energy-regenerating system. In most of the experiments, the volume of the reaction chamber was macroscopic so that the reaction was effectively unbound and the expressed proteins were released to the solution and thereafter sampled. The contribution of nonspecifically adsorbed genes to protein biosynthesis is three to four orders of magnitude lower than that of genes specifically immobilized at maximum packing and surface coverage. We also demonstrate the capture of proteins from crude cell extracts onto micrometer-scale localized antibody affinity traps.[10] Miniaturized traps for newly synthesized proteins could be an important step for developing self-organized protein circuits and enzyme scaffolds. Generic protein traps are also required for miniaturizing the recently introduced self-assembled protein arrays[10,12] from millimeter to micrometer scale. We show that our gene-expression biochip platform can be combined with microfluidic (MF) devices made of elastomers. In this configuration the reaction chambers have volumes of a few nanoliters with heights as low as a few micrometers. We expressed enhanced green fluorescence protein (eGFP) from genes immobilized on a single pad and observed the accumulation of eGFP in the chamber with time. The combination of photolithographic immobilization

of molecules with microfluidic devices allows for the transport of biosynthetic products and reagents by flow, which may have practical implications for parallelism and high throughput. Finally, we demonstrate the embedding of a simple cell-free gene circuit on a chip, with a two-stage cascade[19] in which the first gene encodes a protein that is the input for the expression of the second one. The two genes were immobilized sequentially a distance apart such that the final output was a result of localized synthesis followed by diffusion of products from one location to another.

2. Results

2.1. Synthesis and Characterization of a Single-Step Photosensitive Biocompatible Monolayer

We will briefly review the surface properties in protein/DNA biochips that are required to achieve spatial resolution, biocompatibility, reproducibility, and high signal-to-noise (S/N) ratios. Micrometer-scale immobilization is mostly achieved by UV photolithography by using photolabile protecting groups,[32–34] an approach that has been extensively optimized for DNA oligonucleotide on-chip synthesis.[3,7,35] Grafted poly(ethylene glycol) (PEG) is known to form a biologically compatible interface[36–39] that prevents nonspecific adsorption of proteins and maintains their activity on the surface in a PEG density and length-dependent manner.[40–46] A stable PEG coating of silicon dioxide surfaces can be accomplished through an intermediate organosilane layer.[33,34] Several molecular interfaces have been constructed in situ from PEG and a photolabile group in a stepwise manner, based on commonly used silanes, such as aminopropyl triethoxysilane (APTS), in which the two ends of the molecule are not inert to each other;[47–50] this leads to irreproducibility and uncontrolled interface construction. This drawback significantly compromises the ability to concurrently fulfill two important requirements, namely, reproducible high S/N ratios of specific immobilization and micrometer-scale precision.[32,33]

We designed a chimera molecule, N_ω-Nvoc-amine-N_α-[3-(triethoxysilyl)propyl]-carboxamide-PEG (**2**, Scheme 1; Nvoc = 6-nitroveratrylmethyloxycarbonyl; known as 'Daisy' for short), that combines the principles of a) self-assembled monolayer formation of organosilanes on silicon dioxide, b) light-directed lithographical deprotection for in situ amide bond formation, and c) the biocompatibility of PEG polymers. The starting material and backbone of Daisy is a bifunctional PEG (3400 Da) to which a trialkoxysilane function is attached at one end and an Nvoc moiety, as an amine-protecting group, is attached at the other end (Scheme 1). Daisy is synthesized and analyzed in bulk solution and can be stored indefinitely in powder form. When a solution of Daisy in toluene is incubated with a silicon dioxide surface, a self-assembled monolayer is formed within a few minutes. Cross reactions that may result in molecular disorder and multilayering cannot occur since the two ends of Daisy do not react with each other.[51] Furthermore, the long PEG backbone minimizes intermolecular polymerization by shielding the reactive siloxane groups. The upper side of the Daisy monolayer displays Nvoc-protected amines, which become available for chemical coupling by UV photodeprotection (Scheme 2). We thus obtain in a single step a biocompatible photosensitive monolayer for light-directed submicrometer immobilization of a variety of biomolecules through peptide bonds by using UV-light photolithography.

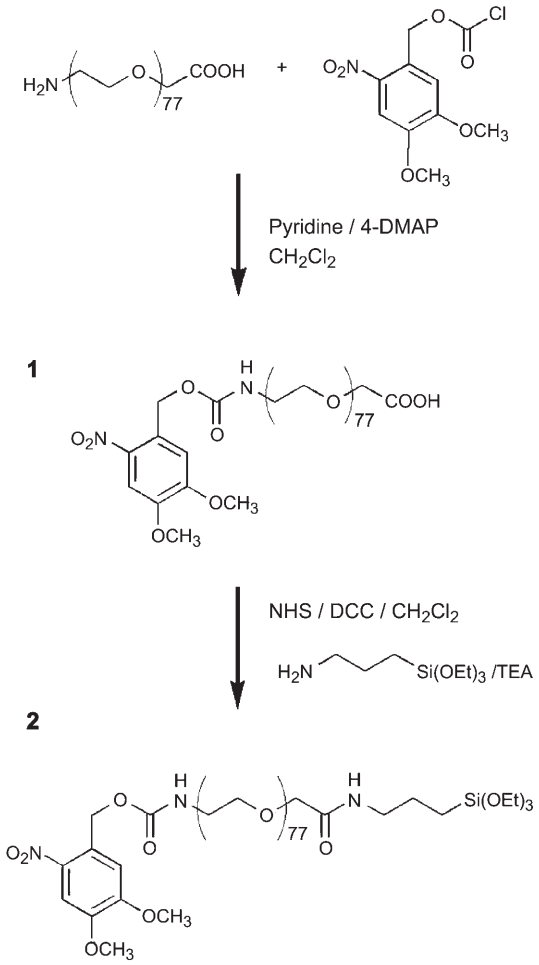

Scheme 1. Two-step synthesis of N_ω-Nvoc-amine-N_α-[3-(triethoxysilyl)-propyl]-carboxamide PEG (**2**; known as 'Daisy'). 4-DMAP: 4-dimethylaminopyridine; DCC: 1,3-dicyclohexylcarbodiimide; NHS: *N*-hydroxysuccinimide; TEA: triethylamine.

To characterize the surface properties, a Daisy layer was deposited on silicon wafers with a 100-nm thickness of thermally grown SiO_2. Atomic force microscopy (AFM), X-ray reflectivity, and ellipsometry analyses were carried out. Surface scans revealed a smooth topography of Daisy-coated substrates with softer features than uncoated ones (see the Supporting Information, Figure S1). Independent of the incubation time (1–60 min), dry Daisy layers were (16.0 ± 0.3) Å thick, with a roughness of (4.0 ± 0.1) Å and an area per molecule of (293 ± 10) Å^2, thereby implying a PEG grafting density of 190 ng cm^{-2}. These data are consistent with a monolayer. The PEG surface density obtained by Daisy deposition is well above the levels required to prevent nonspecific adsorption of proteins.[43,52]

NANO MICRO small

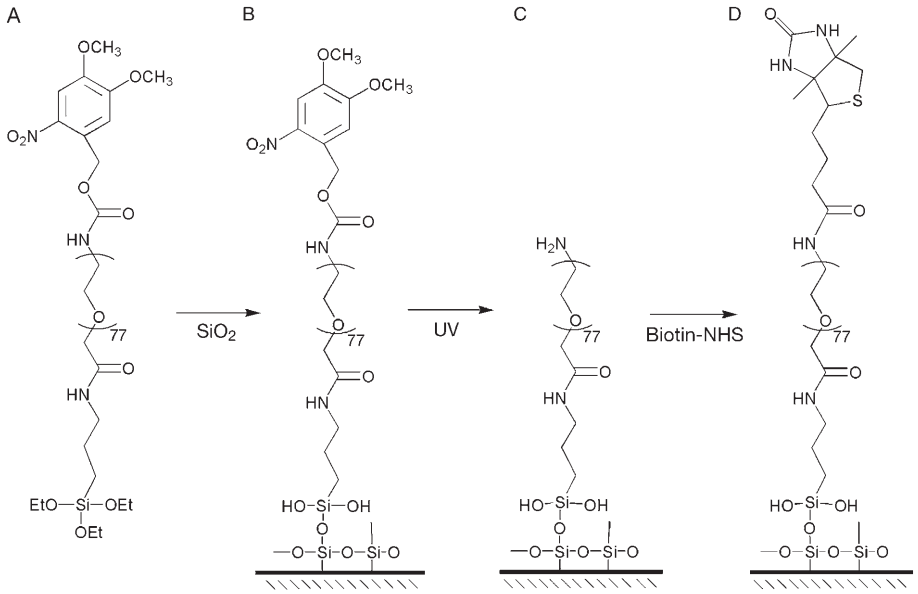

Scheme 2. A) Incubation of Daisy on an SiO_2 surface; B) formation of the monolayer; C) photodeprotection of amines with 365 nm UV light; D) NHS–biotin conjugation.

2.2. Photolithography, Biomolecule Immobilization, and Control of Molecular Density

Photodeprotection was done by using the 365-nm I line of a mercury lamp and a standard fluorescence optical microscope. A pattern was printed on a transparency paper mask placed at the field stop of the fluorescent-light path. The mask was demagnified and imaged on the Daisy layer through the microscope objective lens.[53] Alternatively, photolithography was done in contact mode by using a mask aligner. The deprotected surface amines were conjugated to biotin (by using biotin *N*-hydroxysuccinimidyl ester; Scheme 2), which then served as an anchor for SA-directed attachment of biotin-conjugated moieties (Figure 1). In general, the coupling of SA to biotin-conjugated moieties was done in solution prior to surface immobilization. Excess unbound molecules were washed off to reveal the desired pattern on the chip. A protocol was developed to conjugate one SA to each biotinylated dsDNA (SA–dsDNA; see the Supporting Information). Figure 1B and C shows micrometer-scale immobilization on surface biotin patterns of fluorescein-tagged SA (SA–FITC; FITC: fluorescein isothiocyanate) and of an approximately 2000 bp long SA–dsDNA fluorescently tagged with Cy3 dye (SA–dsDNA–Cy3). Sequential immobilization of different biotin-conjugated molecules on the same chip was done by exchanging the mask, displacing the patterning area, and repeating the process (Figure 1C).

The density of patterned molecules was tuned by varying the intensity and duration of the UV-light pulse through the field-stop aperture and a 60× objective lens (shown in Figure 2A with SA–FITC). At low UV flux only partial deprotection occurred, whereas excess flux most likely damaged the layer and resulted in a halo around the exposed aperture. An optimal contrast was obtained with an intermediate flux value of $\approx 1\ J\,cm^{-2}$. We found that the surface density of immobilized 2000 bp dsDNA was linear with a UV flux of up to $0.5\ J\,cm^{-2}$ and a S/N ratio of ≈200 (Figure 2B). The surface density of a 2000 bp dsDNA layer, which was immobilized on a Daisy-coated chip after exposure of $2\ J\,cm^{-2}$ of 365 nm UV radiation, was estimated by measuring on-chip UV absorption at 260 nm (Figure 2B, inset, and the Experimental Section). We found an average distance of 30 nm between neighboring molecules, which implies tight packing beyond the 400 nm end-to-end coil-size radius.[54] Working in the region where the Daisy interface responds linearly with UV flux allows control of the molecular density with a single exposure of photolithography by using a grayscale mask. A grayscale image was transferred to a sensitive photographic film, which was then used as a mask for photolithography of biotinylated dsDNA conjugated to SA–FITC (SA–FITC–dsDNA). The grayscale mask was thereby translated into a variable density pattern of dsDNA (Figure 2C).

2.3. Protein Microtraps

Daisy-coated chips were tested for the trapping of affinity-tagged proteins from crude cell extracts onto immobilized antibodies. Microtraps for tagged proteins synthesized in vitro were designed based on the interaction between an antibody and the HA peptide tag (amino acid sequence YPYDVPDYA). A plasmid for cell-free expression of eGFP–HA fusion was constructed. A monoclonal biotinylated antibody against the HA peptide tag was patterned on a chip in an array of $10 \times 10\ \mu m^2$ squares after SA immobilization as described above. A cell-free protein-synthesis reaction of eGFP–HA was carried out in solution and then incubated with the immobilized antibody chip. Despite a concentration of ≈ 10–$100\ mg\,mL^{-1}$ of endogenous proteins in the cell extracts, a pattern of eGFP–HA was retained after washing; this demonstrates both specific protein localization and resistance to nonspecific adsorption from crude extracts (Figure 1D).

2.4. On-Chip Protein Biosynthesis

We tested the functionality of our platform for on-chip protein biosynthesis from immobilized dsDNAs expressing the *luciferase* reporter gene (*T7-luc*) in the T7/wheat germ

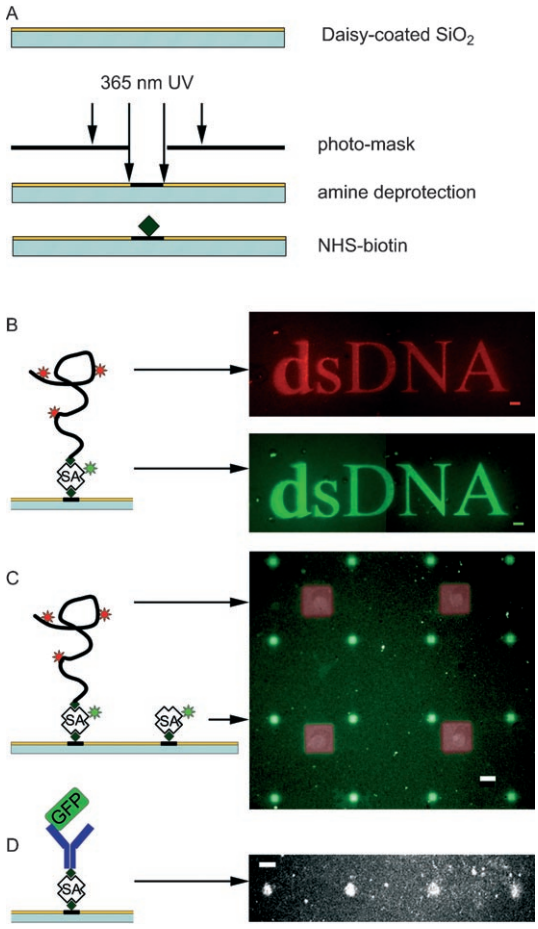

Figure 1. Light-directed localization of SA, genes, and protein traps. A) Schematic representation of the photolithography. Exposure of the Daisy monolayer to 365-nm UV light through a mask deprotects the surface amines for amide bond formation. We couple NHS–biotin as a localization signal pattern for SA. B) A 'dsDNA' pattern was used to immobilize SA–FITC attached to biotinylated 2000 bp dsDNA tagged with Cy3 dye. C) Two sequential steps of photolithography performed on the same chip show the SA and SA–dsDNA patterns separately. Scale bars represent 10 μm. D) A pattern of HA-tagged eGFP from crude cell extracts obtained by immobilizing a biotinylated antibody to the HA tag. The scale bar represents 20 μm.

system.[19] The dsDNAs were oriented on the chip with the promoter close to the surface with an upstream spacer of 200 bp and transcription directed outward from the surface into solution. On the solution side, a flanking spacer of 200 bp was left downstream of the gene. The genes were immobilized on nine regions, each 3 mm in diameter, on a single silicon dioxide chip ($18 \times 18\ mm^2$). Nine parallel luciferase biosynthesis reactions were carried out separately on the chip by using a custom-made device (Figure 3A) in an open configuration with a macroscopic volume (10 μL) of extract bathing each region. Aliquots of the extracts were sampled to measure the luminescence of luciferase released to the solution after a few hours of incubation. In this configuration no imaging was required and luciferase was measured over a wide range of concentrations down to 10^{-14} M in 1–10 μL.

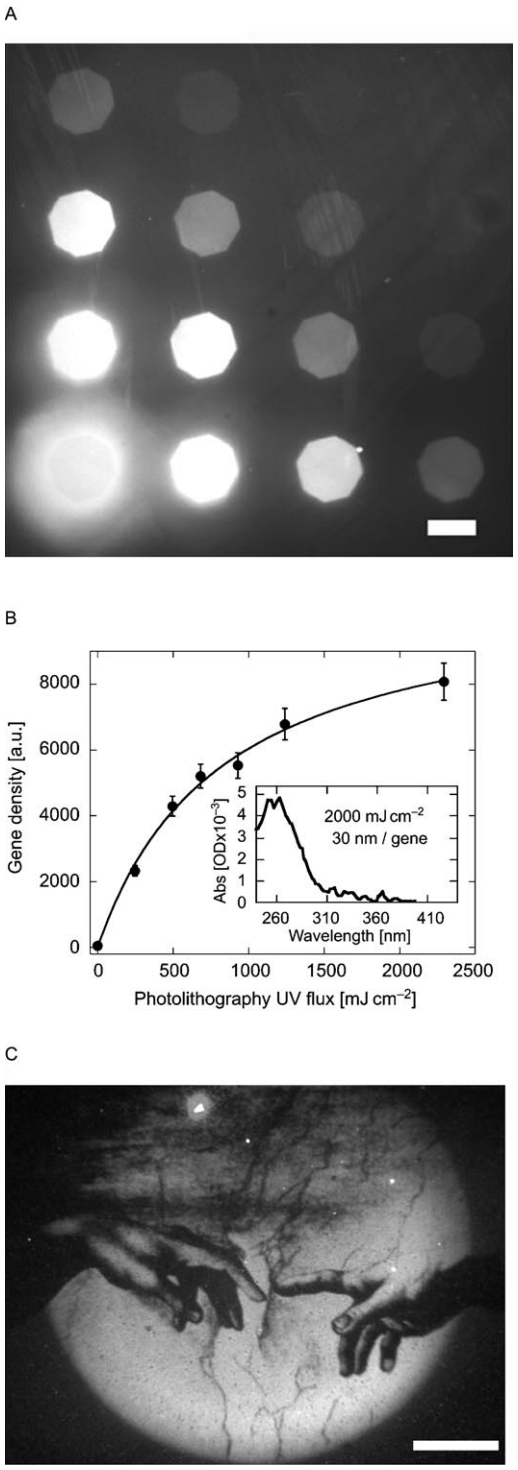

Figure 2. Control of DNA density. A) SA–FITC patterned on a Daisy-coated glass slide through an octagonal mask at various UV light intensities (horizontal axis (right to left): 0.44, 4.4, 18.7, and 70 mW cm^{-2}) and durations (vertical axis (top to bottom): 5 s, 30 s, 2 min, and 10 min). B) Density of 2000 bp dsDNAs as a function of UV flux measured by SA–FITC–dsDNA. Inset: The absorption spectrum of 2000 bp dsDNA immobilized on a Daisy-coated quartz chip, which was exposed to 2 J cm^{-2} UV flux, amounts to an average distance between dsDNA molecules of 30 nm. C) Grayscale fluorescence image of Michelangelo's "Creation of Adam" fresco on a Daisy-coated glass with SA–FITC conjugated to 2000 bp dsDNA. Scale bars represent 50 μm.

NANO MICRO small

Two experiments were carried out to evaluate the efficiency of genes and the dynamic range of protein synthesis on the chip. In the first experiment, we fixed the gene density to its maximal value and varied the extent of surface coverage, thereby controlling gene number. A single chip was exposed to UV light through a photolithographic contact-mode mask divided into nine regions of 5×5 mm^2 in size. In each region, the pattern was an extended two-dimensional (2D) lattice of 10×10 μm^2 units with a fixed lattice constant, L, which varied from 0–400 μm between regions. After dsDNA immobilization on the chip, these patterns correspond to dsDNA surface coverage from 100% down to 0.06% (at fixed density; Figure 3B). Expectedly, luciferase synthesis from these surfaces was maximal for $L = 0$ (100% coverage) and decreased uniformly until $L \approx 200$ μm (0.5–1% coverage). At low surface coverage, with $L \approx 200$–400 μm between repeat units, there was only residual protein synthesis from nonspecifically immobilized SA-conjugated genes, with 250-fold lower yield compared to that with full surface coverage. We compared the relationship between immobilized gene number and protein synthesis at fixed gene density with that of genes in solution. For this, we assumed an average distance between immobilized genes of 30 nm, as measured by UV absorption (Figure 2B), and estimated the effective gene concentration, as if the genes were dispersed in solution. The estimated effective concentration of genes immobilized on a fully deprotected region is ≈1 nM in a 10 μL volume of extract placed on top. Indeed, Figure 3C shows that, similarly to protein biosynthesis from genes in solution, where protein yield is proportional to DNA concentration, protein yield on the chip was proportional to gene surface coverage, although with a somewhat reduced yield compared to solution. This is true only above a threshold value above 10 pM effective gene concentration, or ≈0.5–1% surface coverage of immobilized genes. Below this threshold protein yield is independent of surface coverage, most likely due to residual nonspecifically bound/adsorbed dsDNA.

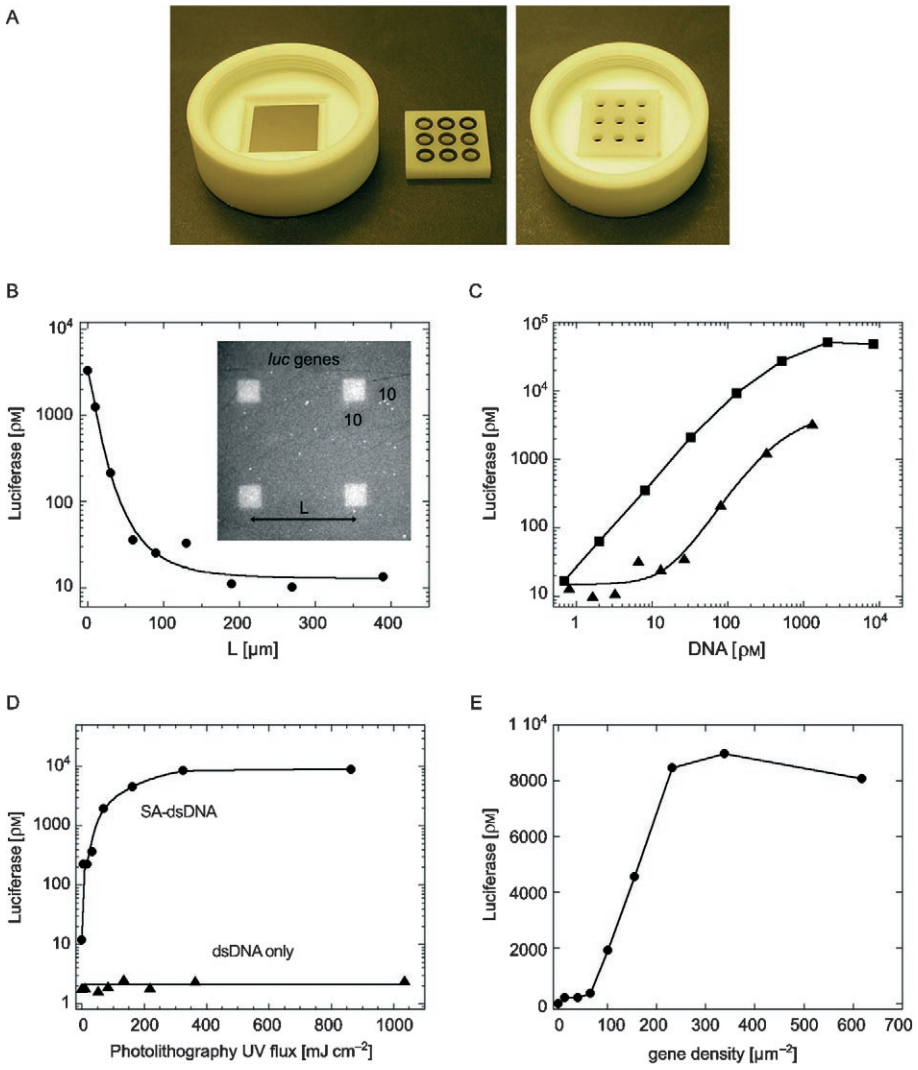

Figure 3. On-chip protein biosynthesis. A) Biochip sample holder for carrying out nine parallel cell-free reactions. The total luciferase yield was measured in solution after 3–4 h of biosynthesis reaction from genes immobilized on Daisy-coated silicon dioxide surfaces. *Luciferase* genes were immobilized on separate regions, each 3 mm in diameter, all on a single chip. The luciferase yield was measured separately in each region. B) Fixed (maximal) gene density at variable surface coverages. Each pattern consisted of the basic 10×10 μm^2 repeat unit arranged in a 2D array at fixed distances ranging from 400–0 μm; thus, coverage varied from 0.06–100% of the surface. Inset: gene immobilization imaged with Cy3-tagged dsDNA (distances in micrometers). C) Luciferase synthesis from genes in solution (squares) and on-chip (triangles) after conversion of the data from (B) into effective gene concentrations. D) Tuning of gene density by using uniform UV exposure (no patterns used) at variable intensity with SA–dsDNA (circles) and dsDNA without SA (triangles). E) Data from (D) plotted versus gene density.

In a second experiment, we controlled the gene number by fixing the UV-exposed area and varied the gene density, rather than fixing the density and varying the UV-exposed area. The nine regions of a chip were exposed uniformly (without a photomask), each at increasing photolithography UV flux to vary the dsDNA density. Two such chips were prepared, one on which we immobilized SA-conjugated

genes and one with the same genes not conjugated to SA. We found that dense SA-conjugated genes produced 700-fold more proteins than sparse ones in the UV-flux range probed, with a steep curve as a function of UV flux, thereby demonstrating a wide dynamic range of protein synthesis on the chip (Figure 3D). Satisfyingly, the control experiment, with genes not conjugated to SA, showed no dependence of protein synthesis on UV flux with only residual protein activity that was ≈5000-fold lower than that of SA-conjugated genes at the maximal density. We then used our UV-flux calibration curve (Figure 2B) to plot the data as a function of gene density (but not fixed gene number; Figure 3E).

2.5. Photolithography of Biomolecules and Protein Biosynthesis within Microfluidic Channels

An MF device made of poly(dimethylsiloxane) (PDMS) elastomer by standard soft lithography[55] was sealed with a Daisy-coated glass cover slip. The coating of Daisy was restricted to a small area of the cover slip (Figure 4A), which allowed the chip to be sealed tightly with the PDMS at its periphery while the photoactivity of Daisy was retained in the center. We immobilized genes coding for *egfp* under T7 RNA polymerase (1200 bp dsDNA) in a small region (24 μm in diameter) by using UV photolithography at the center of a reaction chamber with a volume of ≈5 nL (Figure 4B). UV photolithography, chemical binding of biotin to the deprotected amines, and immobilization of SA–dsDNA were carried out inside the sealed chambers with the device mounted on a microscope and reagents injected under hydrostatic pressure through thin tubing. The transcription/translation reaction was then introduced into the device to synthesize eGFP from the localized genes. We could image synthesis of eGFP only above a concentration of ≈5 nM due to autofluorescence of the extract. Figure 4 shows time-lapse images and continuous kinetics of on-chip eGFP expression and diffusion.

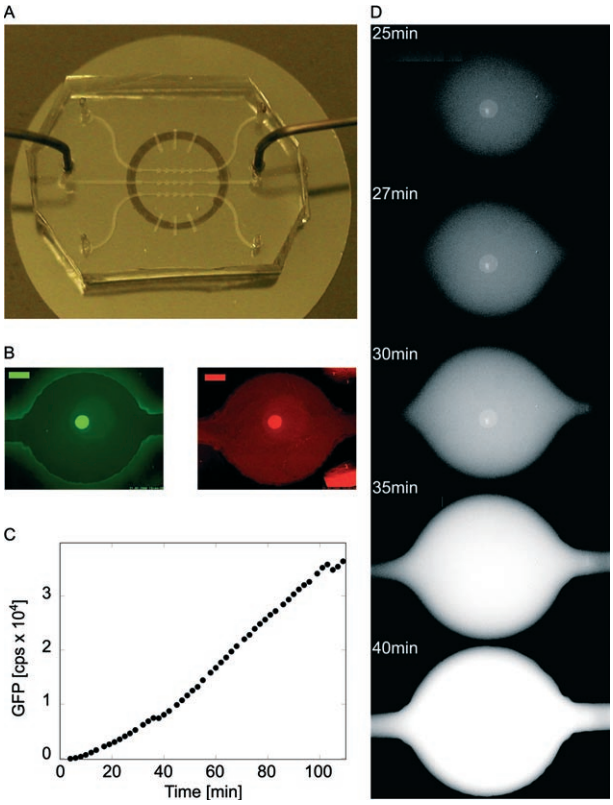

Figure 4. A microfluidic device integrated with the biochip platform. A) A PDMS device composed of connected chambers made by standard soft lithography was sealed by a Daisy-coated glass cover slip. The coating was restricted to a small area of the cover slip (9 mm in diameter; marked black circle). B) UV photoactivation of a small region (24 μm in diameter) on the chip was carried out in a single chamber under the microscope. Chemical binding of biotin to the deprotected amines followed by coupling of SA-conjugated genes coding for eGFP under T7 RNA polymerase (dsDNA, 1200 base pairs) was done by continuous flushing of molecules through the inlets. Fluorescence labeling: SA–FITC conjugated to DNA (green), one protein per DNA, as well as direct end labeling of DNA by Cy5 (red). The scale bar represents 50 μm. C, D) The kinetics of localized on-chip eGFP synthesis followed by its diffusion outwards was monitored after injecting wheat germ coupled transcription/translation extract into the device. The graph in (C) shows the integrated fluorescence intensity over ≈1/2 of the total area of the chamber and located at its center.

2.6. On-Chip Two-Stage Gene Cascade

The Daisy platform is suitable for carrying out complex biochemical functions in which biosynthetic products on the chip cascade from one location to another and interact by reaction–diffusion. To demonstrate this, we sequentially immobilized, in close proximity on a chip, two gene constructs that encode a simple gene circuit:[19] The protein encoded by the first gene, *T7 RNA polymerase* under the SP6 promoter (3100 bp), is the input required to drive expression of the second gene, *luciferase* under the T7 promoter (Figure 5A). The first gene construct was immobilized on 33 dense parallel long stripes, 150 μm apart and each 20 μm wide and 1.2 mm long (Figure 5B). The second gene construct was immobilized on an identical striped pattern displaced by 50 μm from the first gene. The overall gene configuration was, therefore, that of 1D alternating stripes of genes. We launched the cascade in a cell-free reaction with SP6 RNA polymerase as the input to initiate transcription/translation of the first gene. As a noncascaded control experiment, we patterned, on a separate chip, only the construct *T7-luc* and initiated expression with T7 RNA polymerase input. As expected, the kinetics of luciferase luminescence showed a characteristic lag time[19] of ≈50 min in the two-stage process, whereas noncascaded expression of luciferase appeared after 10 min. We estimated the amount of genes immobilized to be 1.3×10^{-15} moles, which is effectively equivalent to a 60 pM concentration in the 20 μL reaction volume placed on top of the chip. The final output of the cascade was 13.2 pM luciferase.

NANO MICRO small

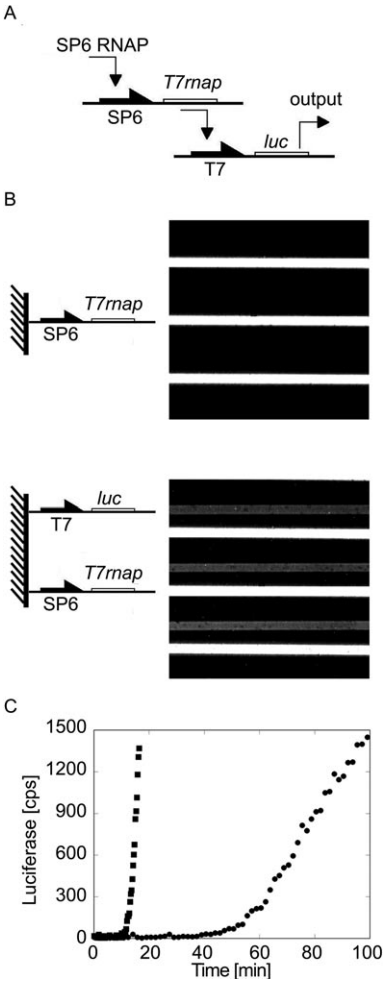

Figure 5. A cell-free two-stage cascade circuit on a chip: A) The SP6 RNA polymerase is the input to initiate transcription/translation of T7 RNA polymerase in a cell-free expression system, which in turn drives firefly luciferase output. B) Photolithography of the gene circuit. A dense striped comb pattern of the output gene (20-μm-wide and 1.2-mm-long stripes; *T7-luc*, 2100 bp) is first immobilized on a glass chip (top). Next, a similar comb pattern of the input gene (*SP6-T7rnap*, 3100 bp) is immobilized in parallel, displaced by 50 μm (bottom). The images correspond to the fluorescence of SA–FITC that is conjugated to dsDNA, one per molecule, as described in the Supporting Information. C) The output of the cascade is measured as a function of time by monitoring the luminescence of luciferase (circles), whereas noncascaded expression of *T7-luc* activated by T7 RNA polymerase input appears after only 10 min (squares).

3. Discussion and Conclusion

3.1. A Single-Step Photolithographic Interface for Entire Genes

We present a robust and simple-to-use biochip platform for active biochips and cell-free biochemical circuits. The method is based on Daisy, a newly designed molecule that forms a self-assembled monolayer on silicon dioxide surfaces and that is photosensitive, biocompatible, and well-suited for localizing a variety of biomolecules (Schemes 1 and 2). We chose a generic and simple conjugation scheme based on biotin–streptavidin coupling. Here we show, for the first time, direct immobilization of entire gene sequences to submicrometer resolution (Figure 1). By tuning the UV flux for photodeprotection we can control the density of genes up to a tight packing of 30 nm between molecules for 2000 bp dsDNA (Figure 2). In general, packing of biomolecules on the chip is expected to depend on their shape, conformation, and charge. This will be reflected in the density versus UV flux calibration curve (Figure 2B). For charged molecules, particularly long dsDNA molecules, salt concentration may alter the packing characteristics and we did not vary this parameter here. Long dsDNA molecules are semiflexible polymers that can attain different conformations when anchored at one point to a surface. We hypothesize that our dsDNA molecules are relaxed coils at low density and become a brush at high density.

The maximal S/N ratio obtained with 2000 bp dsDNA is ≈200 (Figure 2B) for immobilization after complete UV exposure relative to no exposure of Daisy. Long dsDNA molecules would tend to adsorb on surfaces that are less preventive than Daisy-coated ones. One can reduce nonspecific adsorption further. Firstly, a residual amount of SA-conjugated moieties would always bind uniformly to Daisy-coated surfaces even without UV exposure due to a small fraction of unprotected amines left over from the initial synthesis of Daisy. The chemical synthesis of Daisy could be slightly improved to ensure that all amines are protected. Alternatively, one could chemically block any unprotected amines prior to lithography. Secondly, once a designated area on the surface has been exposed to UV light and conjugated with biotin, the subsequent binding of dsDNA molecules could be done under conditions of competition by mixing SA–dsDNA and dsDNA without SA and carefully calibrating the kinetics and concentrations relative to the available surface-conjugated biotins. This procedure will probably improve the S/N ratio, especially when the designated area is only a small fraction of the overall surface.

3.2. On-Chip Protein Expression

We demonstrated on-chip protein biosynthesis from localized genes with very satisfying S/N ratios over a wide dynamic range (Figure 3). The genes were grafted with the promoter close to the surface and transcription progressing towards the solution side. This orientation was preferred over the reversed one in order to increase the propensity for release of newly synthesized transcripts and proteins into the solution. It would be interesting to investigate whether dsDNA orientation affects gene expression as this may be due to crowding, cooperative behavior, and charge distribution close to the surface. The experiments described in Sections 2.4. and 2.6. were done in an open configuration in which the vertical dimension is essentially unbound. Under such conditions the large reaction volume serves as a reservoir for a fresh supply of enzymes and nutrients as well as a sink for byproducts.

Luciferase expression as a function of gene density (but not fixed gene number; Figure 3E) shows a characteristic

S-shaped curve that is steeper than luciferase expression as a function of gene number (Figure 3C), a result implying that gene density affects protein synthesis. Even for the low-density point on the curve with ≈ 10 genes μm^{-2}, the average distance between genes is ≈ 300 nm, which is already within the range of the relaxed gene end-to-end radius of ≈ 400 nm.[54] This suggests a possible scenario in which gene overlap on the chip facilitates enhanced efficiency in the dilute regime and, conversely, reduced efficiency at dense packing. The steep relationship between protein yield and gene density opens the possibility of investigating the utility of genes under controlled conditions of 2D crowding in comparison to their efficiency in solution.

The extent to which translation is colocalized with transcription is, as yet, an open question, which has implications for obtaining spatial patterns of gene expression. A steady-state concentration gradient of synthesized molecules from a localized source will decay over a characteristic length scale of $(D\tau)^{1/2}$, with diffusion constant D and lifetime τ. The lifetime could be tuned by introducing degradation machinery in the extract.[18] If transcripts release from the surface before translation begins, proteins will be synthesized in solution and hence surface-localized genes will not act as intense sources of proteins. In a eukaryotic cell extract (wheat germ lysate), the transcription and translation are less coupled than they are in a prokaryotic one (*Escherichia coli* lysate). Therefore, it is likely that immobilized genes are better localized sources of proteins when expressed in a prokaryotic system than a eukaryotic one and it would be interesting to compare the extent of transcription/translation colocalization in both expression systems.

A different configuration for on-chip gene expression than the one presented here could be investigated by confining the vertical dimension and effectively creating a 2D system. Under such conditions the concentration of dsDNA would be much higher than that attainable in bulk solution with all the biosynthetic reaction components colocalized with the dsDNA. A feeding reservoir attached to the chamber through a membrane might be necessary to prolong expression.[17,56] A transition from on-chip gene expression in 3D to 2D is likely to have a measurable effect, which could be studied by varying the vertical dimensions by using a MF chamber as presented in Section 2.5. More generally, the combination of the Daisy platform with MF technology opens numerous applications for high-throughput proteomics and miniaturized production lines based on cell-free protein biosynthesis,[57] whereby localized parallel reactions could be handled and reagents transported by flow controlled with, for example, MF valves or multiplexers.

3.3. Towards Self-Assembled Microtraps and On-Chip Circuits

We demonstrated the immobilization on a chip of micrometer-scale traps for specific proteins in crude extracts. The traps were based on high-affinity antibody/fusion-peptide interactions.[10] In this experiment the protein fused to the affinity tag was trapped on the surface only after being expressed from genes in solution. The next step would be to coimmobilize a trap in close proximity to the gene, express the protein on the chip, and obtain a physical linkage between genotype and phenotype. This would be important for self-assembled miniaturized protein chips, for in vitro evolutionary studies, and for self-organized circuits of enzymes and scaffolds.

Finally, the simple two-stage cell-free circuit demonstrated here proves the concept of on-chip biochemical circuits. This is a step in the direction of self-organized artificial biological systems. To fully explore this reaction–diffusion process we need to carry out experiments with varied distances between genes and different geometrical layouts, which is beyond the scope of this paper. Nevertheless, we can infer that the time lag is due both to reaction kinetics and to diffusion of products. The cascade realized on the chip showed a 50 min time lag, which is slightly longer than the time lag of 40 min observed in solution (not shown). The difference in the time lags accounts for diffusion between the two sites.

4. Experimental Section

Chemical synthesis: All reactions were conducted under a nitrogen atmosphere and in darkness. Anhydrous dichloromethane, pyridine, and diethyl ether were purchased from Aldrich, TEA was distilled from CaH_2, and ω-amino-α-carboxyl PEG (M_W = 3400; Shearwater Polymers, Inc.) was dried by azeotropic distillation with benzene.

N_ω-*Nvoc-amine*-α-*carboxyl PEG* (***1***): A solution of ω-amino-α-carboxyl PEG (500 mg, 0.15 mmol) in CH_2Cl_2 (8 mL) was treated with 4-DMAP (20 mg) and pyridine (196 mg, 2.48 mmol). The mixture was stirred for 5 min and a solution of 6-nitroveratryl chloroformate (200 mg, 0.73 mmol) in CH_2Cl_2 (4 mL) was added. The reaction vessel was flushed with N_2, sealed, and stirred for 4 days at room temperature. The solvent was evaporated, the residue was dissolved in a minimum amount of CH_2Cl_2, and the desired product **1** was crystallized by slow addition of cold ethyl ether (525 mg, 98%). ^{1}H NMR (250 MHz, $CDCl_3$): $\delta = 3.63$ (m, 278H), 3.95 (s, 3H), 3.98 (s, 3H), 5.52 (d, 2H, $J = 5.6$ Hz), 7.02 (m, 1H), 7.71 (m, 1H).

N_ω-*Nvoc-amine*-N_α-*[3-(triethoxysilyl)propyl]-carboxamide PEG* (***2***): A solution of product **1** (500 mg, 0.14 mmol) in CH_2Cl_2 (20 mL) was treated with DCC (90 mg, 0.44 mmol) and NHS (50 mg, 0.44 mmol). The mixture was stirred overnight at room temperature and the precipitated urea was removed by filtration. The filtrate was treated with 3-aminopropyltriethoxysilane (97 mg, 0.44 mmol) followed by TEA (45 mg, 0.44 mmol) and the resulting mixture was stirred overnight at room temperature. The solvent was evaporated and the residue was dissolved in a minimum amount of CH_2Cl_2 and precipitated with cold dry diethyl ether. Product **2** (200 mg) was recovered and the yield of derivatization was 60%. ^{1}H NMR (250 MHz, $CDCl_3$): $\delta = 1.22$ (t, 5H, J = 7 Hz), 3.64 (m, 278H), 3.96 (s, 3H), 3.99 (s, 3H), 5.53 (d, 2H, $J = 7.6$ Hz), 7.04 (m, 1H), 7.71 (m, 1H). Daisy aliquots were stored in powder form under dry conditions to avoid self-polymerization of the reactive silanes.

NANO MICRO small

Surface modification: Silicon wafers (<100> with a thermally grown oxide layer of 100 nm; MEMC electronic materials, Inc.) and glass cover slips were treated with 5:1:1 proportions of double-distilled water, 25% ammonium hydroxide, and 30% hydrogen peroxide (unstabilized). The wafer-containing solution was heated to 70 °C for 15 min to clean the surfaces and make them hydrophilic. The wafers were washed thoroughly with double-distilled water and were dried by using nitrogen gas. Daisy (0.2 mg) was dissolved in toluene (1 mL; analytic grade) and the solution was filtered with a 0.2-μm filter (Fluoropore, Millipore) in a stainless syringe (Swinney Stainless 13 mm, Millipore). Each previously cleaned substrate was immersed in Daisy solution and incubated for ≈30 min. The surfaces were then rinsed and immersed in toluene for 1 h to remove excess unbound Daisy.

Atomic force microscopy (AFM): Silicon wafers (<100> with a thermally grown oxide layer of 100 nm) were scanned by using a multimode Nanoscope IIIa VEECO-DI (Santa Barbara, CA) AFM instrument in tapping mode and 280–400 kHz resonance frequency silicon probes (Olympus OTESP). AFM images were scanned in air under ambient laboratory conditions.

X-ray reflectometry (XRR): XRR measurements were conducted by using the X23B beam line of the Brookhaven National Laboratories Synchrotron (experiments performed by Prof. P. Dutta and Dr. G. Evmenenko from Northwestern University) in a four-circle Huber diffractometer in specular reflection mode. The reflected intensity was measured as a function of the scattering vector component, $q_z = (4\pi/\lambda)\sin\theta$, perpendicular to the reflecting surface. Incident X-ray energy was 10 keV ($\lambda = 1.240$ Å) and the beam size was 0.4 mm vertical and 2 mm horizontal. Samples were kept under slight helium overpressure during the measurements in order to reduce the background scattering from the ambient gas and radiation damage. Measurements were performed at room temperature. Off-specular background was measured and subtracted from specular counts.

Spectroscopic ellipsometry: Daisy film thickness was measured by using a variable angle spectroscopic ellipsometer (WVASEE32; J. A. Woollam Co.). Measurements were conducted at 70° incidence angle with 390–900 nm white light. To deduce the film thickness we took into account the thermally grown 100-nm SiO_2 layer on the silicon <100> wafer and a PEG layer with a refractive index of 1.460 at 632.8 nm.[58]

UV photolithography, optical microscopy, and florescence imaging: Imaging and UV photolithography by projection were carried out on standard optical microscopes (Axiovert 200M, Zeiss, and BX51-WI, Olympus) equipped with standard mercury arc lamps. A (365 ± 10)-nm band-pass filter (Chroma) for the I line was used for photodeprotection. Masks were printed on transparency paper, placed in a custom-made holder between two glass cover slips, and placed in the position of the epifluorescence field stop for imaging onto Daisy-coated chips. Images were recorded by using a sensitive QE-Sensicam (PCO) camera. Lithography was also done in contact mode on a mask aligner configured for the I line (MA-6, Karl-Suss) by using a chrome-on-quartz mask.

On-chip UV/Vis absorption: The absorption spectrum of dsDNA molecules (2000 bp) immobilized on Daisy-coated quartz slides (University Wafers, 5 × 15 mm^2) was measured by a UV/Vis spectrometer (Varian Cary 50 probe). Absorption spectra were taken first after coupling of NHS-biotin as a background measurement and then after immobilization of SA–dsDNA. The absorption peak that appeared at 263 nm in the subtracted spectrum corresponds to the grafted dsDNA layer contribution and gave an optical density (OD) of 4.8×10^{-3}. The surface density of dsDNA molecules was extracted by using the relationship in Equation (1), where $\varepsilon = 2.64 \times 10^7\ M^{-1}\,cm^{-1}$ is the extinction coefficient of 2000 bp dsDNA at 260 nm, A_{260} is the absorption at that wavelength, and γ is the molecular surface density.

$$\gamma = 6 \times 10^6 \left(\frac{A_{260}}{\varepsilon}\right) \text{molecules}\,nm^{-2} \quad (1)$$

Biotinylation of deprotected surface amines: Coupling of *N*-hydroxysuccinimidobiotin (Sigma) was done in 270 mM borate buffer (pH 8.35) for 2 h after filtration (Whatman Puradisc 25 AS 0.45 μm filters) and then extensively washed, first with 1 M NaCl and then with 20 mM tris(hydroxymethyl)aminomethane (Tris) buffer (pH 7.5) and 150 mM NaCl.

Immobilization of biomolecules: SA (10–100 nM) and SA–dsDNA (30 nM) were incubated for 0.5–2 h on the chip after biotinylation of deprotected surface amines in 20 mM Tris buffer (pH 7.5) and 150 mM NaCl. Extensive washing was done with the same buffer and with double-distilled water. For the trap experiment, biotinylated anti-HA antibody, (0.5 $\mu g\,mL^{-1}$ in phosphate-buffered saline (PBS), Roche), was incubated with a pattern of SA on the surface for 2 h and rinsed extensively with PBS.

Parallel protein biosynthesis on a chip: Daisy-coated silicon dioxide substrates (18 × 18 mm^2) were placed in a custom-made teflon reaction chamber (Figure 3A). A special spacer with nine O-rings separated the nine regions, thereby allowing cell-free reaction mix (10 μL) to be placed on top of each region on the chip. Cell-free coupled transcription/translation reactions were carried out by using the TNT T7-Coupled Wheat Germ Extract System (Promega) according to the manufacturer protocol. Aliquots were taken from each region on the chip to measure luciferase luminescence.

Luciferase assay: Luminescence from the luciferase cell-free synthesis reaction mixture (2 μL) from the chip added to luciferase assay reagent (18 μL; Roche) was measured on a luminometer made of a photon-counting unit (H7155, Hamamatsu), a counter (53131A 225 MHz, Agilent), and a homemade sample holder. For real-time measurements of luciferase biosynthesis we added 1 μL of luciferase assay reagent to every 9 μL of cell-free reaction mixture. Luminescence was converted to concentration by using a calibration curve obtained with recombinant luciferase (Promega).

Two-gene cascade on a chip: Round cover glasses (25-mm diameter; Deckglaser) were mounted inside custom-made Teflon holders. In this configuration, a 5-mm inner diameter Viton O-ring restricted a small reaction area where genes were immobilized. A cell-free coupled transcription/translation reaction mix (18 μL; TNT SP6-Coupled Wheat Germ Extract System (Promega)) was placed on the glass. Mineral oil (5 μL) was placed on top of the reaction mix to reduce convection. The SP6 RNA polymerase concentration was reduced to a third of the concentration recommended by the manufacturer.

Microfluidic device fabrication: The MF device was fabricated by using a standard soft-lithography technique.[55] Molds were

made from SU-8-100 negative photoresist (Microchem), with a crosslinker-to-elastomer ratio of 1:10. The channel height was 100 μm. Channels were prepared by casting of PDMS elastomer (Sylgard-184, Dow-Corning) on the mold and curing it at 80 °C for 40 min. After separation of the cured PDMS from the mold and punching of holes at the inlets and outlets, the PDMS was irreversibly attached to a Daisy-coated cover slip glass that constituted the channel floor. The cover slip was previously coated with Daisy only in a restricted region of 9 mm in diameter by using a custom-made sample holder. After attachment, the device was cured at 80 °C for 2 h.

Acknowledgements

We thank T. Beatus, S. Daube, D. Fass, M. Lahav, L. Nissim, V. Noireaux, J. Sagiv, R. Tenne, M. Van Der Boom, and M. Wilchek for useful discussions and comments and P. Dutta and G. Evmenenko for carrying out the X-ray reflectivity measurements. R.B.-Z. is an incumbent of the Beracha Foundation Career Development Chair. This research was supported by the Israel Science Foundation.

[1] M. Schena, D. Shalon, R. W. Davis, P. O. Brown, *Science* **1995**, *270*, 467.
[2] D. Lockhart, H. Dong, M. Byrne, M. Follettie, M. Gallo, M. Chee, M. Mittmann, C. Wang, M. Kobayashi, H. Horton, E. Brown, *Nat. Biotechnol.* **1996**, *14*, 1675.
[3] S. Fodor, J. Read, M. Pirrung, L. Stryer, A. Lu, D. Solas, *Science* **1991**, *251*, 767.
[4] A. Pease, D. Solas, E. Sullivan, M. Cronin, C. Holmes, S. Fodor, *Proc. Natl. Acad. Sci. USA* **1994**, *91*, 5022.
[5] G. MacBeath, S. Schreiber, *Science* **2000**, *289*, 1760.
[6] H. Zhu, J. Klemic, S. Chang, P. Bertone, A. Casamayor, K. Klemic, D. Smith, M. Gerstein, M. Reed, M. Snyder, *Nat. Genet.* **2000**, *26*, 283.
[7] G. H. McGall, F. C. Christians, *Adv. Biochem. Eng./Biotechnol.* **2002**, *77*, 21.
[8] J. LaBaer, N. Ramachandran, *Curr. Opin. Chem. Biol.* **2005**, *9*, 14.
[9] G. V. Shivashankar, S. Liu, A. Libchaber, *Appl. Phys. Lett.* **2000**, *76*, 3638.
[10] N. Ramachandran, E. Hainsworth, B. Bhullar, S. Eisenstein, B. Rosen, A. Y. Lau, J. C. Walter, J. LaBaer, *Science* **2004**, *305*, 86.
[11] G. Jung, G. Stephanopoulos, *Science* **2004**, *304*, 428.
[12] M. He, M. Taussig, *J. Immunol. Methods* **2003**, *274*, 265.
[13] D. S. Tawfik, A. D. Griffiths, *Nat. Biotechnol.* **1998**, *16*, 652.
[14] J. W. Szostak, D. P. Bartel, P. L. Luisi, *Nature* **2001**, *409*, 387.
[15] M. M. Hanczyc, S. M. Fujikawa, J. W. Szostak, *Science* **2003**, *302*, 618.
[16] I. A. Chen, R. W. Roberts, J. W. Szostak, *Science* **2004**, *305*, 1474.
[17] V. Noireaux, A. Libchaber, *Proc. Natl. Acad. Sci. USA* **2004**, *101*, 17669.
[18] V. Noireaux, R. Bar-Ziv, J. Godefroy, H. Salman, A. Libchaber, *Phys. Biol.* **2005**, *2*, P1.
[19] V. Noireaux, R. Bar-Ziv, A. Libchaber, *Proc. Natl. Acad. Sci. USA* **2003**, *100*, 12672.
[20] M. Isalan, C. Lemerle, L. Serrano, *PLoS Biol.* **2005**, *3*, 488.
[21] J. Kim, K. S. White, E. Winfree, Mol. Syst. Biol. **2006**, *2*, 68.
[22] J. Kim, E. Winfree, J. Hopfield, *Adv. Neur. Inf. Proc. Syst.* **2004**, 681.
[23] Y. Benenson, B. Gil, U. Ben-Dor, R. Adar, E. Shapiro, *Nature* **2004**, *429*, 423.
[24] N. C. Seeman, *Trends Biochem. Sci.* **2005**, *30*, 119.
[25] S. P. Liao, N. C. Seeman, *Science* **2004**, *306*, 2072.
[26] T. Liedl, M. Olapinski, F. C. Simmel, *Angew. Chem.* **2006**, *118*, 5129; *Angew. Chem. Int. Ed.* **2006**, *45*, 5007.
[27] W. U. Dittmer, F. C. Simmel, *Nano Lett.* **2004**, *4*, 689.
[28] B. Yurke, A. J. Turberfield, A. P. Mills, F. C. Simmel, J. L. Neumann, *Nature* **2000**, *406*, 605.
[29] P. Yin, H. Yan, X. G. Daniell, A. J. Turberfield, J. H. Reif, *Angew. Chem.* **2004**, *116*, 5014; *Angew. Chem. Int. Ed.* **2004**, *43*, 4906.
[30] J. Bath, S. J. Green, A. J. Turberfield, *Angew. Chem.* **2005**, *117*, 4432; *Angew. Chem. Int. Ed.* **2005**, *44*, 4358.
[31] A. Eldar, R. Dorfman, D. Weiss, H. Ashe, B. Z. Shilo, N. Barkai, *Nature* **2002**, *419*, 304.
[32] P. Kumar, S. Agarwal, K. Gupta, *Bioconjugate Chem.* **2004**, *15*, 7.
[33] D. Shin, K. Lee, K. Janga, J. Kim, W. Chung, Y. Kim, Y. Lee, *Biosens. Bioelectron.* **2003**, *19*, 485.
[34] D. Nivens, D. Conrad, *Langmuir* **2002**, *18*, 499.
[35] G. McGall, A. Barone, M. Diggelmann, S. Fodor, E. Gentalen, N. Ngo, *J. Am. Chem. Soc.* **1997**, *119*, 5081.
[36] S. Metzger, M. Natesan, C. Yanavich, J. Schneider, G. Lee, *J. Vac. Sci. Technol. A* **1999**, *17*, 2623.
[37] L. Ruiz-Taylor, T. Martin, F. Zaugg, K. Witte, P. Indermuhle, S. Nock, P. Wagner, *Proc. Natl. Acad. Sci. USA* **2001**, *98*, 852.
[38] D. Falconnet, A. Koenig, T. Assi, M. Textor, *Adv. Funct. Mater.* **2004**, *14*, 749.
[39] D. Falconnet, D. Pasqui, S. Park, R. Eckert, H. Schift, J. Gobrecht, R. Barbucci, M. Textor, *Nano Lett.* **2004**, *4*, 1909.
[40] C. Palegrosdemange, E. Simon, K. Prime, G. Whitesides, *J. Am. Chem. Soc.* **1991**, *113*, 12.
[41] S. Jeon, J. Andrade, *J. Colloid Interface Sci.* **1991**, *142*, 159.
[42] S. Jeon, J. Lee, J. Andrade, P. DeGennes, *J. Colloid Interface Sci.* **1991**, *142*, 149.
[43] H. Du, P. Chandaroy, S. Hui, *Biochim. Biophys. Acta* **1997**, *1326*, 236.
[44] H. Lu, C. Campbell, D. Castner, *Langmuir* **2000**, *16*, 1711.
[45] Z. Yang, J. Galloway, H. Yu, *Langmuir* **1999**, *15*, 8405.
[46] P. Harder, M. Grunze, R. Dahint, G. Whitesides, P. Laibinis, *J. Phys. Chem. B* **1998**, *102*, 426.
[47] W. Bascom, *Macromolecules* **1972**, *5*, 792.
[48] F. Boerio, L. Armogan, S. Cheng, *J. Colloid Interface Sci.* **1980**, *73*, 416.
[49] E. Plueddemann, *J. Adhes. Sci. Technol.* **1991**, *5*, 261.
[50] D. Kurth, T. Bein, *Langmuir* **1995**, *11*, 3061.
[51] R. Maoz, L. Netzer, J. Gun, J. Sagiv, *J. Chim. Phys. Phys.-Chim. Biol.* **1988**, *85*, 1059.
[52] S. Sofia, V. Premnath, E. Merrill, *Macromolecules* **1998**, *31*, 5059.
[53] J. Love, D. Wolfe, H. Jacobs, G. Whitesides, *Langmuir* **2001**, *17*, 6005.
[54] F. Valle, M. Favre, P. De Los Rios, A. Rosa, G. Dietler, *Phys. Rev. Lett.* **2005**, *95*.
[55] D. C. Duffy, J. C. McDonald, O. J. A. Schueller, G. M. Whitesides, *Anal. Chem.* **1998**, *70*, 4974.
[56] A. S. Spirin, V. I. Baranov, L. A. Ryabova, S. Y. Ovodov, Y. B. Alakhov, *Science* **1988**, *242*, 1162.
[57] T. Sawasaki, T. Ogasawara, R. Morishita, Y. Endo, *Proc. Natl. Acad. Sci. USA* **2002**, *99*, 14652.
[58] S. Sharma, R. Johnson, T. Desai, *Appl. Surf. Sci.* **2003**, *206*, 218.

Received: September 12, 2006
Published online on February 7, 2007

